

Quark Loop Effects with an Improved Staggered Fermion Action *

C. Bernard ^a, T. Burch ^b, T.A. DeGrand ^c, C.E. DeTar ^d, Steven Gottlieb ^e, U.M. Heller ^f,
K. Orginos ^b, R.L. Sugar ^g, and D. Toussaint ^b,

^aDepartment of Physics, Washington University, St. Louis, MO 63130, USA

^bDepartment of Physics, University of Arizona, Tucson, AZ 85721, USA

^cPhysics Department, University of Colorado, Boulder, CO 80309, USA

^dPhysics Department, University of Utah, Salt Lake City, UT 84112, USA

^eDepartment of Physics, Indiana University, Bloomington, IN 47405, USA

^fCSIT, Florida State University, Tallahassee, FL 32306-4120, USA

^gDepartment of Physics, University of California, Santa Barbara, CA 93106, USA

We have been studying effects of dynamical quarks on various hadronic observables, using our recently formulated improvement for staggered fermions. To illustrate improvement, we show that the light hadron spectrum in the quenched approximation gives remarkably good scaling. We highlight three new results: (1) We find no apparent quark loop effects in the Edinburgh plot with 2+1 flavors of dynamical quarks at $a = 0.14$ fm. (2) We show that dynamical quarks modify the shape of the heavy quark potential. (3) We present results hinting at meson decay effects in light hadron spectroscopy.

1. INTRODUCTION

Recent proposals for Symanzik improvement of the staggered fermion action have produced encouraging results, particularly in an improved flavor and rotational symmetry [1,2]. Adding a few terms to the conventional Kogut-Susskind action, namely three-link, five-link and seven-link staples and a third-neighbor coupling, removes all tree-level $\mathcal{O}(a^2)$ errors [3–9]. The computational price for using this action is quark mass dependent, and is roughly a factor of 2.5 for the lightest masses we are using. Here we extend previous work with our preferred “Asqtad” action, studying scaling in the quenched approximation, and exploring the effects of dynamical quarks on the light hadron spectrum and the heavy-quark potential.

We have accumulated a library of gauge configurations, both quenched (one-loop Symanzik improved gauge action) and dynamical.¹ Our

$m_{u,d} / m_s$	$10/g^2$	size	lats.	a/r_1
quenched	8.40	$28^3 \times 96$	101*	0.2683(9)
	8.00	$20^3 \times 64$	408	0.3753(8)
	7.75	$16^3 \times 32$	206	
	7.60	”	100	
	7.40	”	191	
0.40 / 0.40	7.35	$20^3 \times 64$	335	0.3757(10)
0.20 / 0.20	7.15	”	349	0.3700(10)
0.10 / 0.10	6.96	”	344	0.3721(13)
0.05 / 0.05	6.85	”	421	0.3732(15)
0.04 / 0.05	6.83	”	208*	0.3751(19)
0.03 / 0.05	6.81	”	474*	0.3749(14)
0.02 / 0.05	6.79	”	368*	0.3762(13)
0.01 / 0.05	6.76	”	128*	0.3848(25)

* sample is currently being enlarged.

dynamical fermion lattices are generated in the presence of two lighter flavors (u , d) and one heavier flavor (s). For the dynamical fermion sample the gauge coupling is tuned so that the lattice

*Presented by C. DeTar.

¹The MILC code, including the improved KS action code,

is publicly available. Gauge configurations are also available. Please contact doug@physics.arizona.edu or de-tar@physics.utah.edu for details

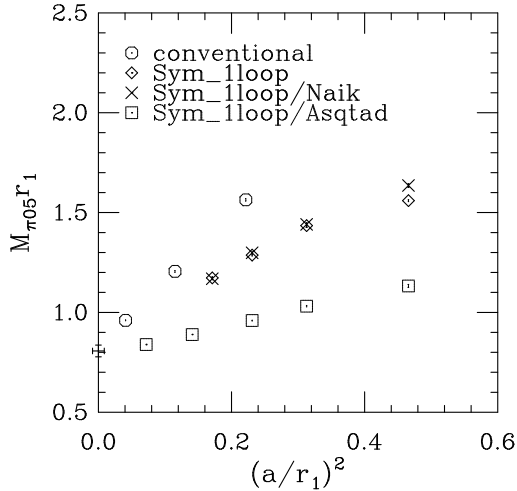


Figure 1. Flavor symmetry test. Mass of the non-Goldstone local pion *vs* lattice spacing in units of r_1 (see text) for progressively improved actions: (octagon) conventional staggered fermion and single-plaquette gauge action, (diamond) same but with an improved gauge action, (cross) same but with the Naik third-neighbor term, and (square) our preferred Asqtad action.

spacing remains the same as the quark mass is varied, allowing an exploration of quark mass effects independent of scale. The current parameter set is shown in the table above.

2. SCALING TESTS

To measure the degree of residual flavor symmetry breaking, we compute the mass of the local non-Goldstone pion (π_{05}) as a function of lattice spacing at a fixed value of the Goldstone pion mass (m_G) on a series of quenched lattices [11]. In particular, we fix $m_G r_1 = 0.807(3)$ (Goldstone π) with the scale r_1 set by the force $F_{Q\bar{Q}\text{static}}$ between static quarks $r_1^2 F_{Q\bar{Q}\text{static}}(r_1) = 1$, a variant of Sommer's scale[10]. The value of r_0/r_1 depends on the quark masses, varying from 1.376(2) for the quenched theory to 1.44(1) for physical quark masses. The effect of improving the fermion action is shown in Fig. 1. It is expected that the curves for all actions extrapolate to the Goldstone

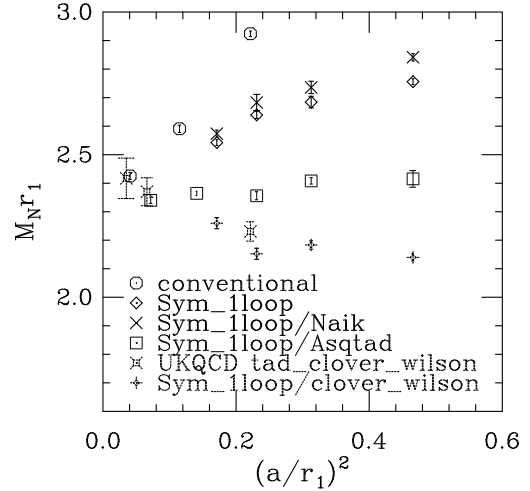


Figure 2. Scaling test. Nucleon mass *vs* lattice spacing. Same as 1, but including Wilson-clover results.

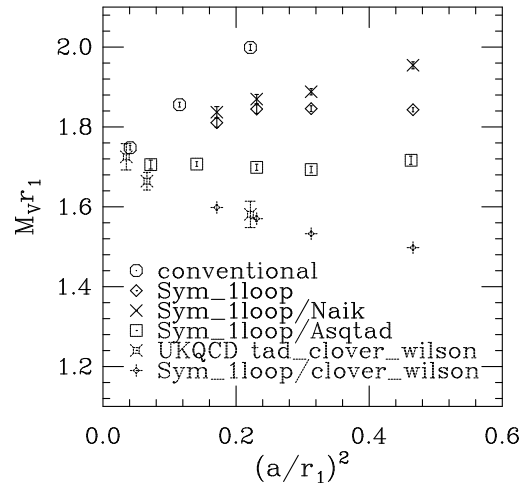


Figure 3. Same as 2, but for the rho meson mass.

pion mass.

Scaling of the ρ and nucleon masses is shown in Figs. 2 and 3. Results for variants of the Wilson-clover action are also shown [12,13]. For these masses, the Asqtad action gives the best result. Nonetheless, it is encouraging that staggered

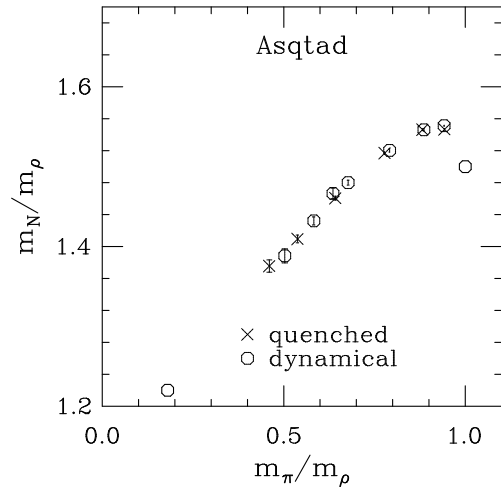


Figure 4. Edinburgh plot comparing results for a quenched and 2 + 1 flavor dynamical simulation at $a = 0.14$ fm. Octagons show the experimental value (lower left) and infinite quark mass value (upper right).

fermion and Wilson-clover simulations agree in the continuum limit.

3. DYNAMICAL QUARK EFFECTS: EDINBURGH PLOT

To determine the effect of dynamical quarks on the light hadron spectrum, we ran a series of quenched and 2+1 dynamical fermion simulations with gauge couplings tuned to fix the lattice spacing $a = 0.14$ fm, using $20^3 \times 64$ lattices for both the quenched and dynamical runs. The plotted points are from the runs described in Table I with light quark masses down to $0.02a^{-1}$ and from the quenched run at $10/g^2 = 8.0$. The resulting Edinburgh plot in Fig. 4 shows no discernible change when dynamical quarks are introduced. This 2+1 flavor $a = 0.14$ fm result appears to be in conflict with our previous claims, based on the conventional action with two sea quark flavors in the $a \rightarrow 0$ limit [16]. We are currently investigating whether the difference comes from the number of flavors, the continuum extrapolation, or some other source of systematic error.

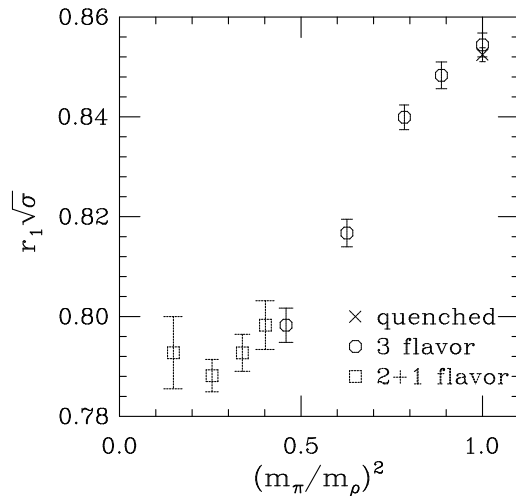


Figure 5. Square root of the string tension in units of r_1 vs the squared ratio of the pion to rho mass. The octagons are done with three degenerate flavors (for $m_q \geq m_s$), while the squares are runs with two light flavors and a fixed strange quark mass.

4. DYNAMICAL QUARK EFFECTS: HEAVY QUARK POTENTIAL

Dynamical quark loops modify the heavy quark potential [17], *e.g.*, by opening the two-meson decay channel and by altering the running of the Coulomb coupling. In Fig. 6 we plot the heavy quark potential with and without 3 flavors of sea quarks of mass $am_q = 0.05$. The vertical scale is adjusted to give agreement at r_1 , and since the force at r_1 is used to set the scale, the two potentials have the same slope there.

To the extent the potential changes shape under the influence of sea quarks, setting the lattice scale from the heavy quark potential clearly has limitations. This point is illustrated in Fig. 5, where we plot the ratio of two possible heavy-quark-potential-inspired scales as a function of the ratio of the pion to rho mass.

5. DYNAMICAL QUARK EFFECTS: MESON DECAY

As the pion mass drops to zero with decreasing quark mass, one expects to see evidence for

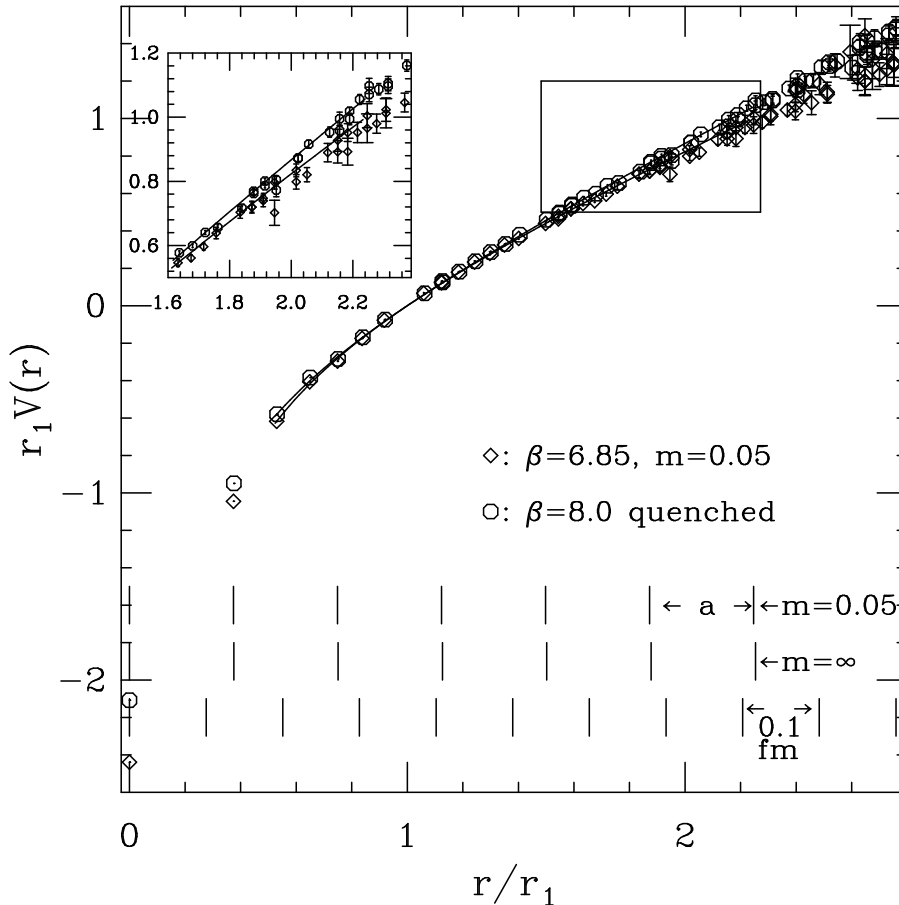


Figure 6. Heavy quark potential with and without $2+1$ flavors of sea quarks. Rulers show lattice and physical units for the two matched simulations.

the decay of heavier mesons, such as $\rho \rightarrow 2\pi$ and $a_0 \rightarrow \eta\pi$. The mixing between a resonant state and a two-meson decay state should result in avoided level crossing in the spectrum of the resonant state. While such decays are natural when dynamical quarks are present, quenched simulations may also show hints of decay in some cases, through “hairpin” diagrams, although at different rates.

Previous attempts to observe effects of meson decay in the ρ spectrum were unsuccessful [18]. Here we report results of a preliminary attempt to observe effects of the decay $a_0 \rightarrow \eta\pi$. This threshold is easier to approach than the $\rho \rightarrow \pi+\pi$ threshold because the final pseudoscalars don’t have to carry away angular momentum, so they

can both be at zero momentum. However, it is difficult, because with staggered quarks the a_0 appears in the same propagators as the pions, so we must extract the alternating exponential from a propagator containing a much larger simple exponential. We measure the a_0 mass (*i.e.* lowest energy in the a_0 (0^{++}) channel) as a function of quark mass. This is done on quenched and dynamical fermion configurations. Preliminary results, shown in Fig. 7, suggest that the lowest 0^{++} mass drops more rapidly with decreasing quark mass in the dynamical fermion simulation. The drop appears to follow the threshold energy of the decay channel, also shown. Such a result would be expected from avoided level crossing. In fact, for the lighter quark masses it is very difficult to

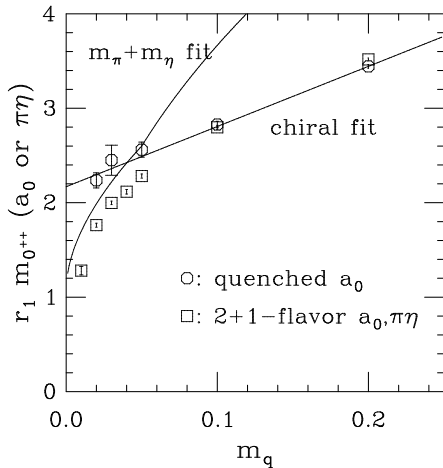


Figure 7. Mass of the 0^{++} state seen in our spectrum analysis *vs* quark mass with and without dynamical quarks. The $\eta - \pi$ threshold is plotted.

extract masses for the quenched a_0 . This may be a signal of the non-unitarized (because of the quenching) couplings to two particle states.

6. SUMMARY

We continue studies using a recently proposed improved staggered fermion action. We find that the light hadron spectrum in our currently preferred Asqtad action scales very well. We have begun a systematic study of quark loop effects with 2 + 1 flavors. Our present sample of gauge configurations has been constructed so that the lattice spacing is kept constant as the quark masses are varied. We see no quark loop effects in the light hadron spectrum with 2 + 1 flavors at a lattice spacing of $a = 0.14$ fm. However, sea quarks evidently modify the heavy quark potential both at short and long distance, suggesting caution in using this potential to set a precision lattice scale at unphysical quark masses. Preliminary determinations of the mass of the a_0 as a function of quark mass suggest evidence for the decay to $\eta + \pi$.

This work is supported by the US National Science Foundation and Department of Energy and used computer resources at Los Alamos National Lab, NERSC, NCSA, NPACI and the University of Utah (CHPC).

REFERENCES

1. K. Orginos, D. Toussaint and R.L. Sugar, Phys. Rev. D **60** (1999) 054503;
2. K. Orginos, R. Sugar and D. Toussaint, Nucl. Phys. (Proc. Suppl.) **83** (2000) 878 [hep-lat/9909087].
3. S. Naik, Nucl. Phys. **B316** (1989) 238.
4. T. Blum *et al.*, Phys. Rev. D **55** (1997) 1133.
5. C. Bernard *et al.*, Phys. Rev. D **58** (1998) 014503.
6. J.F. Lagäe and D.K. Sinclair, Nucl. Phys. (Proc. Suppl.) **63** (1998) 892; Phys. Rev. D **59** (1999) 014511.
7. K. Orginos and D. Toussaint, Phys. Rev. D **59** (1999) 014501; Nucl. Phys. B (Proc. Suppl.) **73** (1999) 909.
8. G.P. Lepage, Nucl. Phys. (Proc. Suppl.) **60A** (1998) 267.
9. G.P. Lepage, Phys. Rev. D **59** (1999) 074501.
10. R. Sommer, Nucl. Phys. **B411** (1994) 839.
11. The MILC collaboration: C. Bernard *et al.*, Phys. Rev. D **61**, (2000) 111502 [hep-lat/9912018].
12. Sara Collins, Robert G. Edwards, Urs M. Heller and John Sloan, Nucl. Phys. (Proc. Suppl.) **53** (1997) 877; private communication.
13. K.C. Bowler *et al.*, Phys. Rev. D **62** (2000) 054506 [hep-lat/9910022].
14. C. Bernard *et al.*, Nucl. Phys. B, (Proc. Suppl.), **63** (1998) 182; Phys. Rev. D **58** (1998) 014503.
15. C. Bernard *et al.* Phys. Rev. Lett. **81** (1998) 3087.
16. C. Bernard *et al.*, Nucl. Phys. B (Proc. Suppl.) **73** (1999) 198.
17. C. Bernard *et al.*, Phys. Rev. **D62** (2000) 034503 [hep-lat/0002028]; S. Aoki, this conference.
18. C. Bernard *et al.*, Phys. Rev. **D48** (1993) 4419. [hep-lat/9305023].